ChemComm

HIGHLIGHT

View Article Online
View Journal | View Issue

Cite this: *Chem. Commun.*, 2025, **61**, 407

Photochemical upcycling of polymers *via* visible light-driven C–H bond activation

Wei Yi,†*[a] Jing Liu†[b] and Xiao-Qiang Hu *[a]

The excessive use and improper disposal of plastics have placed a significant burden on the environment. To mitigate this impact, prioritizing the chemical upcycling of plastics is crucial. Unlike traditional thermochemical upcycling, which requires harsh conditions such as high temperatures and pressures, photochemical upcycling is viewed as a more environmentally friendly and cost-effective alternative. This includes using light to promote C–H bond activation to achieve the oxidative degradation of plastics, generating various valuable small molecules, or employing light-induced C–H bond activation for post-polymerization modification of post-consumer plastics to obtain polymers with enhanced properties. These methods are highly attractive approaches within the realm of chemical upcycling. This mini-review highlights the scientific breakthroughs in upcycling polymers through oxidative degradation and post-polymerization modification *via* visible light-driven C–H bond activation. In addition, the reaction mechanism compatibility as well as practical application have been emphatically discussed.

Received 2nd November 2024,
Accepted 26th November 2024

DOI: 10.1039/d4cc05866f

rsc.li/chemcomm

Introduction

Plastics are convenient, inexpensive, and durable materials that have become deeply embedded in various aspects of human life through years of extensive use.[1] They are widely applied across numerous fields such as packaging, electronics, construction, medicine, textiles and many other fields. However, the excessive use and improper disposal of plastics have created a significant burden on the environment. The statistics on plastic pollution are alarming. Plastic production rose from 320 million tons in 2015 to 430 million tons in 2023, and it is expected to double by 2050, leading to a global per capita plastic consumption of 84.37 kg per year. A considerable portion of this production is designed for single-use applications, with less than 10% being recycled.[2] It is estimated that between 19 to 23 million tons of plastic end up in lakes, rivers, and oceans each year, with single-use plastics discarded or incinerated posing threats to human health and biodiversity, directly harming the entire ecosystem.[3] Moreover, plastic products consume energy and emit greenhouse gases throughout their entire lifecycle, from production and manufacturing to recycling and disposal, exacerbating the climate crisis. In 2015, plastic-related greenhouse gas emissions were estimated at 1.7 billion tons of carbon dioxide equivalent, and this figure is projected to increase to approximately 6.5 billion tons of carbon dioxide equivalent by 2050, accounting for 15% of the global carbon budget.[4] As plastic continues to exert a significant influence on daily life, it simultaneously poses serious environmental challenges. Consequently, there is an urgent need for effective recycling and repurposing of plastic materials.

Nowadays, the plastic wastes can be recycled through mechanical reprocessing and chemical upcycling.[5] Mechanical reprocessing entails the collection of plastic waste, which is then ground into flakes or pellets for use in creating new plastic products, all while maintaining the original chemical structure.[6] This method is appreciated for its simplicity and efficiency; however, it can result in a decline in the quality of the final products due to issues such as polymer degradation, contamination, and physical wear during the processing stages.[7] In contrast, chemical upcycling refers to the process of converting low-value or waste plastics into higher-value materials or products through chemical reactions.[8] Unlike mechanical recycling, which merely reprocesses plastics into similar forms, chemical upcycling breaks down plastic polymers into their fundamental monomers or other valuable chemicals. This process can involve various methods, such as pyrolysis,[9] depolymerization,[10] or hydrolysis,[11] allowing the recovery of raw materials that can be used to create new plastics, fuels, or other chemicals. The key benefits of chemical upcycling include the potential to convert difficult-to-recycle plastics into useful products, reduce environmental pollution,

[a] *Key Laboratory of Catalysis and Energy Materials Chemistry of Ministry of Education & Hubei Key Laboratory of Catalysis and Materials Science, School of Chemistry and Materials Science, South-Central Minzu University, Wuhan 430074, China. E-mail: hxq071303127@126.com, huxiaoqiang@mail.scuec.edu.cn, chmweiyi@163.com*

[b] *Wuhan Institute of Photochemical Technology, Wuhan 430080, China*

† These authors contributed equally to this work.

and create opportunities for a circular economy by transforming waste into valuable resources. For example, through chemical upcycling, plastics such as polyethylene and polypropylene can be converted into basic chemicals (*e.g.*, ethylene, propylene) or more complex organic molecules, which can serve as new raw materials for synthesizing other products. This transformation not only enhances the economic value of the materials but also promotes resource reuse. The circular economy emphasizes the closed-loop utilization of resources to minimize waste generation. Within this framework, technologies for photochemical upcycling can help achieve the reuse of plastics, reducing the need for new materials. By converting waste plastics into useful chemicals, companies can achieve resource recycling while minimizing environmental impacts.

In recent years, methods for upcycling plastics using catalytic processes have gained great attention, primarily through thermocatalytic[12] and photocatalytic approaches.[13] Unlike thermochemical methods such as pyrolysis, which typically demand significant energy and operate under extreme conditions like high temperatures and pressures,[14] photocatalysis is regarded as a more environmentally friendly and cost-effective alternative.[15] This is due to its ability to function under mild conditions at ambient pressure and temperature, utilizing sunlight or low-energy artificial light sources like LEDs. Additionally, while thermocatalysis often involves harsh conditions, photocatalysis allows for the gentle activation of specific chemical bonds while preserving other functional groups, enabling a high degree of selectivity for desired products.[16]

Photocatalytic oxidative degradation of polymers[17] is a prime example of chemical upcycling, as it transforms polymers into valuable oxidized molecules by activating the C–H bonds in the polymer backbone. This process facilitates the cleavage of polymer chains in the presence of oxygen through photo-induced hydrogen atom transfer (HAT) catalysis.[18] Likewise, through the activation of C–H bonds, C–H functionalization of polymers involves the incorporation of additional functional groups while preserving the integrity of the C–C bonds in the polymer backbone. This technique, commonly applied to virgin polymers and referred to as post-polymerization modification,[19] can be considered a form of chemical upcycling when it transforms post-consumer plastics into new polymers of higher value. With the rapid advancements in photocatalysed C–H activation of small molecules in recent years,[20] numerous studies on photochemical oxidative degradation and post-polymerization modifications utilizing C–H activation have emerged, facilitating the chemical upcycling of post-consumer plastics. Recently, there are some reviews that summarize polymer degradation[21] and polymer modification.[22] For example, the Kokotos group reported a review focusing on photochemical upcycling protocols for the degradation of polymer categories, ranging from polystyrene to polyacrylate-based polymers.[23] While, there remain very few that specifically address photochemical upcycling, particularly in terms of recent advancements in photochemical oxidative degradation of polymers and photochemical polymer modification from the perspective of C–H activation approaches.

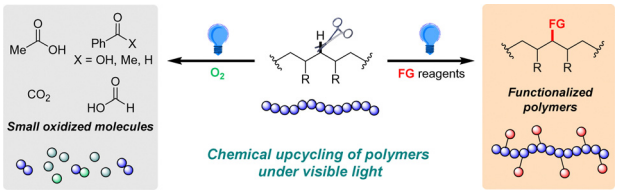

Scheme 1 Chemical upcycling of polymers *via* visible light-driven C–H bond activation.

In this review, we aim to summarize the recent strategic advances in the burgeoning field of photochemical upcycling, focusing on two types of reactions: photochemical oxidative degradation and photochemical C–H functionalization of polymers *via* C–H bond activation (Scheme 1). Meanwhile, this review will also highlight the development, outlook, and challenges of this emerging field. Notably, this work will not include discussions on heterogeneous photocatalyst-promoted polymer upcycling and photoreforming as a few recent reviews have already addressed this topic.[24]

Photochemical C–H functionalization of polymers *via* C–H bond activation

Post-polymerization modification (PPM) is an appealing strategy for converting low-cost polymers into functional materials. This approach takes advantage of the high-volume production of these plastics while introducing functionality that is randomly distributed along the polymer backbone. In addition, the advancement of PPM techniques aimed at boosting the value of both post-industrial and post-consumer polymers could serve as a foundational approach for upcycling plastic waste. In 2018, Leibfarth and co-workers reported a visible light-driven approach for radical-mediated C–H xanthylation, which allows for the regioselective functionalization of branched polyolefins without leading to simultaneous scission of the polymer chains.[25] After subjecting an trifluorotoluene solution of poly(ethylethylene) (PEE) with M_n = 3.6 kg mol^{-1} and $Đ$ = 1.26 in the presence of *N*-xanthylamide (1 equiv. per repeat unit) under blue LED light illumination (450 nm) for 19 hours at room temperature, the polyolefin was successfully functionalized, achieving the C–H xanthylation with level of up to 18 mol%. Importantly, the functionalization of PEE at 60 °C was just as effective in the neat state as it was in trifluorotoluene at 25 °C. Following xanthylation, the gel permeation chromatography (GPC) demonstrated an increase in both the number average (M_n) and weight average (M_w) molecular weights because of introduction of xanthate groups. Of note, the molecular weight distribution (MWD) remained relatively unchanged, suggesting the excellent chemoselectivity of this approach. By harnessing the remarkable versatility of alkyl xanthates in both radical-mediated and polar bond-forming reactions, xanthylated polyolefins can be considered as a material platform for creating diverse functional materials that unlock a wide array of new polymer properties.

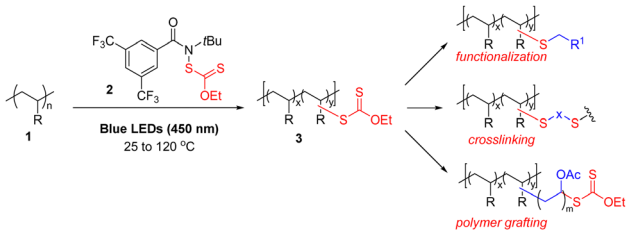

Scheme 2 Visible light-driven C–H xanthylation of polymers.

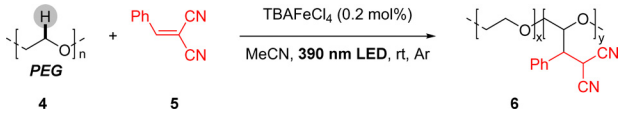

Scheme 3 C–H alkylation of polyethers *via* iron photocatalysis.

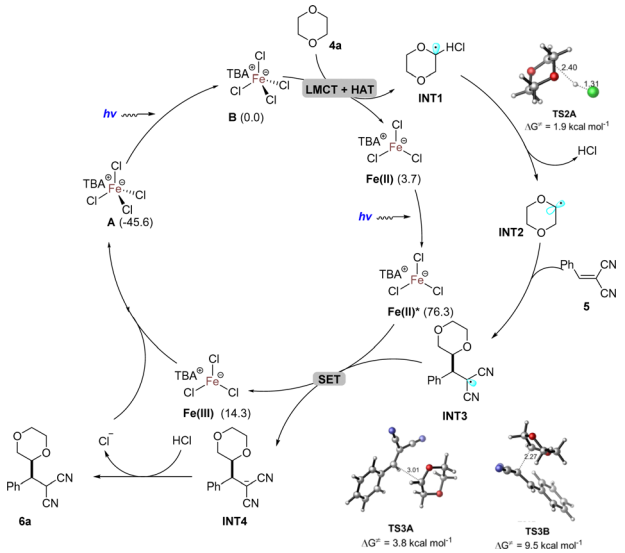

Scheme 4 Possible mechanism for C–H alkylation of polyethers *via* iron photocatalysis.

As illustrated in Scheme 2, xanthated PEE can be converted into a range of valuable functionalized polyolefins through processes such as functionalization, crosslinking, and polymer grafting. The selectivity of this approach, governed by the reagent, can inhibit the formation of tertiary radicals in the polymer backbone, which are known to compromise material properties.[26] Commercial polymers such as polyethylene (PE), high-density polyethylene (HDPE), linear low-density polyethylene (LLDPE), and hyperbranched polyethylene were regioselectively xanthylated, achieving up to 8 mol% xanthylation with only 10 mol% loading of *N*-xanthylamide **2**. For both PEE and HDPE, the polymers were xanthylated at comparable levels, with no signs of chain scission observed.

The iron-catalysed photoinduced ligand-to-metal charge transfer (LMCT) strategy[27] has recently emerged as a powerful method for the C–C bond cleavage[28] and functionalization of C(sp^3)–H bonds.[29] This approach generates chlorine radicals that initiate intermolecular hydrogen atom transfer (HAT) processes, triggering a series of subsequent functionalization reactions. In this context, Zeng and co-workers disclosed a method for controllable C–H bond alkylation of polyethers with electron-deficient alkenes under mild conditions through photoinduced iron catalysis.[30] Under LED light (390 nm) irradiation, the iron-catalysed C–H functionalization of polyethylene glycols (PEG 6000) with electron-deficient alkene **5** in MeCN allows for controlled and selective production of alkylation products with varying levels of functionalization, reaching a maximum level of 19.8 mol%. Reducing the reaction concentration to 0.5 or 0.2 M can suppress chain cleavage and allow for better control over the molecular weight (M_w) and dispersity ($Đ$) value. Under standard conditions, PEGs with diverse terminal groups, along with polytetrahydrofuran (PTHF), polypropylene glycol (PPG), and PEG–PPG–PEG, could be efficiently functionalized. To illustrate the significant synthetic potential of the iron-catalysed alkylation approach, the authors prepared novel hydrogels from PEG-6000 and maleic anhydride. The modified polyethylene oxide (PEO) containing dinitrile groups were then utilized as solid-state electrolytes, resulting in enhanced lithium ionic conductivities (Scheme 3).

An extensive density functional theory (DFT) calculation was carried out to examine the proposed mechanism, using the reaction of dioxane with compound **5** as a model system. The Gibbs energy profile calculated for the iron catalytic cycle is presented in Scheme 4. Upon light excitation, catalyst **A** was converted to catalyst **B**, requiring an endothermic energy of 45.6 kcal mol^{-1}. Following this, catalyst **B** undergoes a LMCT process, resulting in the formation of **Fe(II)** and a chlorine radical. This chlorine radical can subsequently abstract a hydrogen atom from 1,4-dioxane through a HAT mechanism, leading to the generation of radical **INT1**. The C–H bond cleavage in **INT1** occurs *via* transition state **TS2A**, which has a small energy barrier of 1.9 kcal mol^{-1}, yielding **INT2** and releasing a molecule of HCl. The regioselectivity of **INT2** in its reaction with alkene **5** was evaluated, revealing that the pathway through transition state **TS3B**, which involves the carbon atom bonded to two cyano groups, is higher in energy by 9.5 kcal mol^{-1}. In contrast, the pathway *via* transition state **TS3A**, associated with the electron-deficient carbon center, has an energy of 3.8 kcal mol^{-1}, making it 5.7 kcal mol^{-1} lower in energy relative to **TS3B**. **Fe(II)** exhibits greater stability, which renders the SET process between **Fe(II)** and **INT3** thermodynamically unfavorable. To promote the subsequent reaction, **Fe(II)** was exposed to a second excitation *via* LED light, resulting in the formation of the photoexcited state **Fe(II)***. The excited state **Fe(II)*** acts as a reductant, facilitating the reduction of **INT3** to **INT4** while concurrently being oxidized to **Fe(III)**. Subsequently, the anion **INT4** undergoes protonation by the HCl generated the desired product **6a**, while the released chloride anion is captured by **Fe(III)**, thus regenerating the catalyst **A** and completing the catalytic cycle.[30]

Using the same strategy, the Zeng group successfully achieved the C–H bond alkylation of polyolefins.[31] The level of functionalization in this reaction can be modulated by

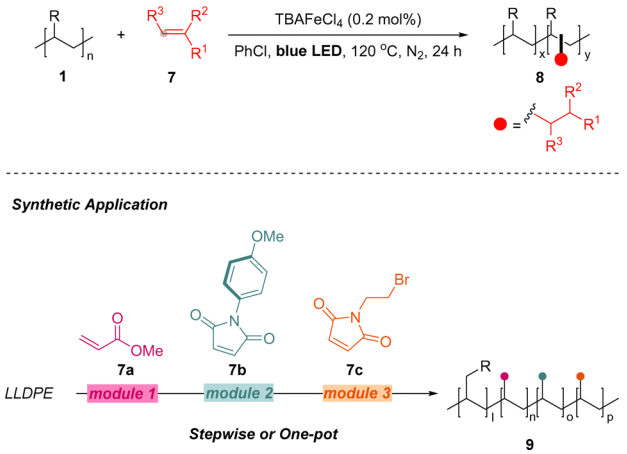

Scheme 5 Photoinduced iron-catalysed C–H alkylation of polyolefins.

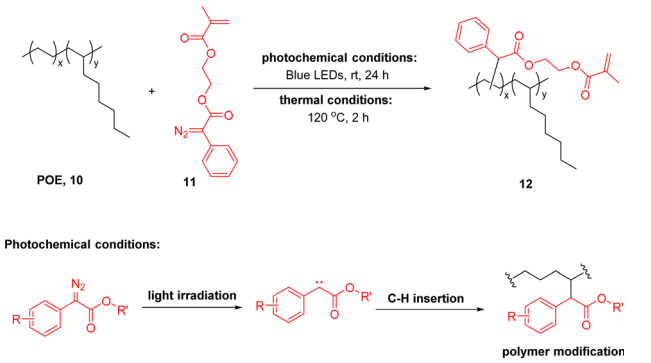

Scheme 6 Carbene-mediated C–H functionalization of polymers.

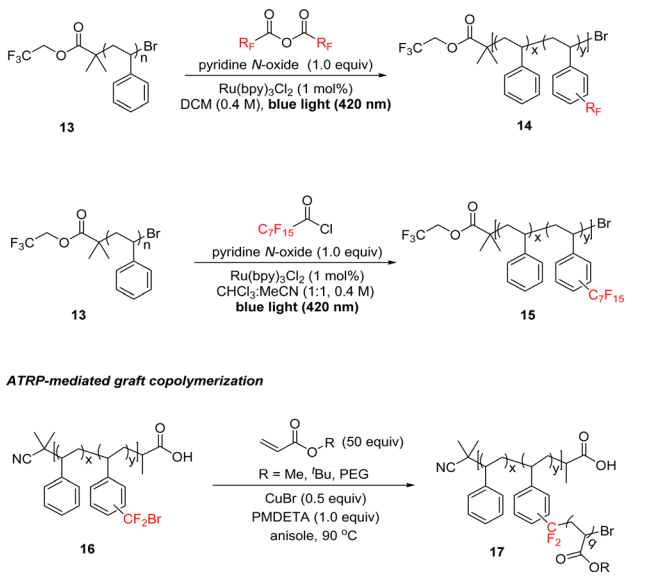

Scheme 7 Photocatalysed C–H fluoroalkylation of aromatic polymers.

adjusting the equivalent of olefins. Under optimal conditions, plastic bags made from high-density polyethylene (HDPE), disposable containers made from polypropylene (PP), and foam boxes made from polystyrene (PS) are all suitable for C–H bond alkylation. Additionally, this method allows for the synthesis of polyolefins containing multi-polar groups through either stepwise or one-pot multiple installations of functional groups (Scheme 5). Furthermore, ionomers and hydrophilic materials can be easily produced from commodity polyethylene with this method, highlighting the significant potential for developing innovative materials.

In addition to the photo-induced HAT strategy, carbene-mediated C–H bond insertion reactions[32] can also be utilized for the functionalization of polymers. Recently, the Pan group presented a novel carbene-mediated post-polymerization modification (PPM) strategy that employs diazo compounds.[33] This reaction can be initiated under either photochemical or thermal conditions. In photochemical conditions, diazo compounds are activated by visible light[34] to extrude nitrogen and generate a carbene intermediate. This intermediate then facilitates the insertion into the C–H bonds of polymer backbones, enabling effective functionalization of commodity polymers with a variety of properties, including hydrophobicity, hydrophilicity, and epoxy modification. For example, this approach can be used to enhance the polarity of polyolefin elastomer (POE), thereby improving its compatibility with polylactic acid (PLA) during blending, which reinforces the mechanical properties of PLA (Scheme 6).

In 2015, Stephenson[35] reported a photocatalytic trifluoromethylation of arenes and heteroarenes using trifluoroacetic acid and its anhydride as CF_3 radical precursor (Scheme 7). Inspired by this work, Leibfarth and his team reported a photocatalytic platform for the C–H functionalization of aromatic polymers.[36] This method utilizes mild reaction conditions to generate electrophilic fluoroalkyl radicals, enabling the fluoroalkylation of a variety of commercially relevant polyaromatic substrates, including both post-industrial and post-consumer plastic waste, while maintaining their otherwise appealing thermomechanical properties. With 1.0 mol% of $Ru(bpy)_3Cl_2$ as the photocatalyst, a 32 ± 2 mol% trifluoromethylation of polystyrene **13** could be accomplished by combining 1.0 equiv. of pyridine N-oxide and 1.1 equiv. of trifluoroacetic anhydride (TFAA) per repeat unit in dichloromethane at room temperature, utilizing 420 nm blue light irradiation. Control experiments showed that both photocatalyst and visible light are essential for this polymer trifluoromethylation. By adjusting the stoichiometry of TFAA and pyridine N-oxide relative to the repeat unit, a tuneable level of C–H trifluoromethylation in the polymer was achieved. In addition to polystyrene, polycarbonates and Eastman's Tritan® copolyester can be functionalized with 14 mol% and 20 mol% incorporation, respectively, using 2.0 equivalents of pyridine N-oxide and 2.2 equivalents of TFAA relative to the repeat unit. Remarkably, post-industrial expanded polystyrene (EPS) foam waste can be upcycled through this polymer trifluoromethylation method, without any significant change in molecular weight distribution (MWD) after functionalization. Furthermore, the incorporation of a bromodifluoromethyl group introduces functionality that acts as an initiator for atom transfer

radical polymerization (ATRP), offering an easy method for the chemical diversification of commodity polymers. Subsequently, the Leibfarth group accomplished this transformation using organic photoredox catalysts as an alternative to $Ru(bpy)_3Cl_2$. In addition to commodity polymer substrates, the metal-free functionalization method was also applicable to post-consumer and post-industrial plastic waste.[37]

Photochemical oxidative degradation *via* C–H bond activation

Photo-induced oxidative degradation is a chemical process in which polymers undergo degradation when exposed to light, particularly UV radiation.[38] This process typically involves the generation of reactive oxygen species (ROS), such as singlet oxygen, superoxide anions, and hydroxyl radicals. These reactive species can interact with polymers, leading to the cleavage of C–C bonds. As the degradation process propagates, the material breaks down into smaller fragments or undergoes alterations in its chemical structure. Given the rapid advancements in visible light-promoted C–H bond activation strategies, researchers are investigating the potential of visible light-induced polymer oxidative degradation as a means to obtain valuable small molecules more efficiently, safely, and selectively, while avoiding the use of ultraviolet light.

In 2022, the Reisner group introduced a mild method for the deconstruction of plastics *via* photocatalytic CEH oxidation of tertiary carbons in the polymer backbone.[39] An ethyl acetate solution of polystyrene (PS) with a molecular weight of 260 000 g mol^{-1} was subjected to blue LED light illumination (450 nm, 14.4 W) for 48 hours, along with 20 mol% fluorenone, 1 equiv. of H_2SO_4, and oxygen balloon, resulting in the successful converting polystyrene into benzoic acid and other aromatic products. Benzoic acid was obtained as the major product with a yield of about 38%. Other aromatic compounds, including ethyl benzoate, acetophenone, benzaldehyde, as well as aromatic oligomers, were identified as by-products using ^1H NMR spectroscopy, HPLC and GC–MS. After 48 hours of reaction, about 95% of the fluorenone photocatalyst remained intact, and the recycled photocatalyst was able to yield 34% of benzoic acid in a subsequent 24-hour reaction.

Control experiments demonstrated that the photocatalyst, light, and acids are essential for this reaction. Additionally, diluted acid was found to be tolerable and resulted in a reasonable yield. To demonstrate the practicality of this approach, a gram-scale reaction was carried out using expanded PS packaging foam ($M_w \sim 250\,000$, PDI ~ 4.2). By extending the reaction time to 72 hours, the yield of aromatic products was comparable to that obtained from pure PS, with 36 ± 2% of benzoic acid included in the total yield. The authors performed a range of mechanistic study, including radical trapping studies, UV-vis absorption measurements, Stern–Volmer analyses and DFT calculation. Specifically, DFT calculations showed that the free energy changes (ΔG) and the kinetic energy barrier ($\Delta G^{\ddagger}$) for the HAT step catalyzed by fluorenone are −24.6 kcal mol^{-1} and +20.3 kcal mol^{-1}, respectively. In comparison, the ΔG for the HAT step in the absence of the photocatalyst is +77.5 kcal mol^{-1}, which clearly demonstrates the catalytic function of fluorenone. Additionally, the $\Delta G^{\ddagger}$ for the β-scission process in the presence of an acid additive is +3.9 kcal mol^{-1}. In contrast, the C–C bond cleavage without the participation of H^+ has a significantly higher $\Delta G^{\ddagger}$ of +66.1 kcal mol^{-1}, highlighting the crucial role of the acid. A stoichiometric amount of acid is employed as a sacrificial reagent to remove H_2O from **INT3** and to facilitate the oxygen reduction reaction.

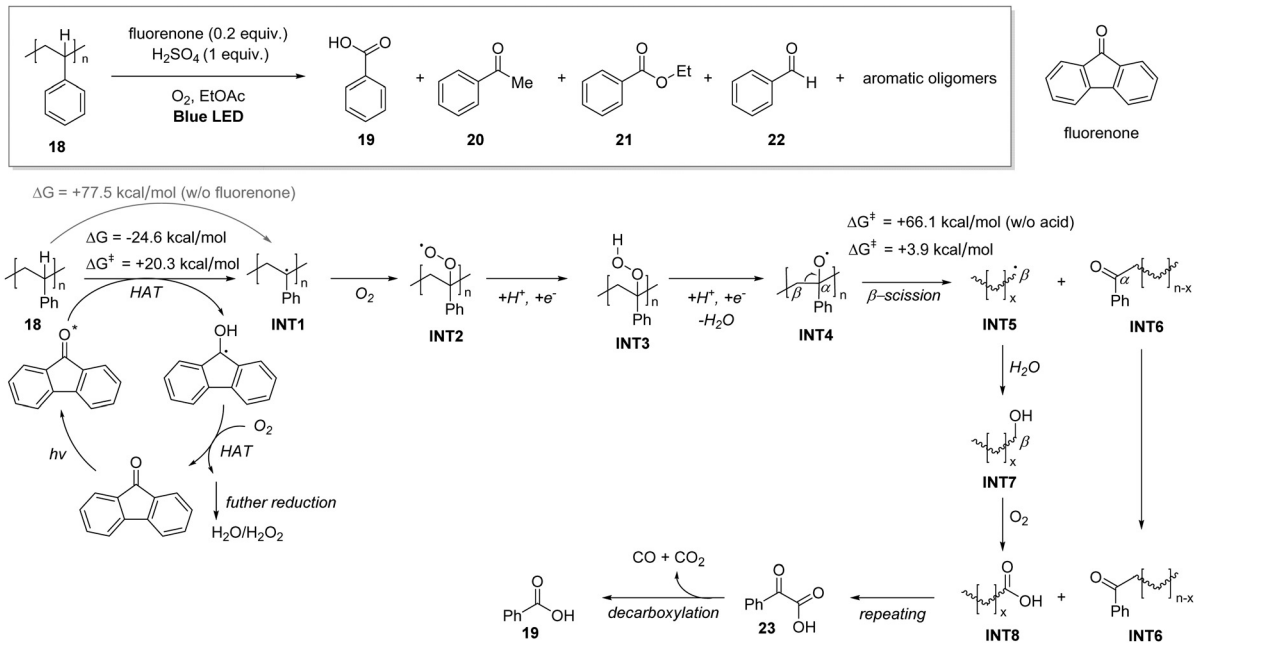

Scheme 8 Photocatalytic deconstruction of polystyrene *via* a C–H oxidation pathway.

According to the results of theoretical calculations and experimental results, a possible mechanism was provided as shown in Scheme 8. The HAT process involving PS and the excited state of the photocatalyst initiates the formation of PS radicals, in addition to a ketyl radical. Following this, O_2 is reduced to regenerate the photocatalyst. The PS radicals are then subjected to oxygenation, leading to the formation of **INT2**. This is succeeded by the HAT reaction of the peroxyl radical, which yields **INT3**, and subsequently, H_2O is eliminated to form **INT4** in the presence of acid. The reaction progresses through an acid promoted β-scission mechanism, generating radical species **INT5** alongside a terminal aromatic C═O group. **INT5** will be oxidized and hydrated to produce alcohol **INT7**, which will undergo further oxidation to form a carboxylic acid. The continuous breakdown through these reactions will ultimately lead to the generation of phenylglyoxylic acid, which can then decarboxylate to yield benzoic acid along with CO_2 and CO. Similarly, by employing aromatic ketones as HAT abstractors, Kokotos and his team achieved the depolymerization of PS in air without the use of acid additives, utilizing anthraquinone photocatalysts.[40] The protocol can be applied to everyday polystyrene-based plastic waste to yield benzoic acid, which can subsequently be converted into pharmaceutical agents like salicylic acid and acetylsalicylic acid.

To develop a practically applicable methods achieving the degradation of PS in a highly selective manner, Xiao and colleagues have disclosed a photoinduced acid catalysed selective aerobic degradation of commercial PS to valuable compounds (Scheme 9).[41] Using *p*TsOH·H_2O (5 mol%) as the catalyst and O_2 (1 bar) as the oxidant, PS (F.W.: 192 000) was converted into formic acid and benzoic acid as the main products in a benzene/CH_3CN (1 : 1, 1 mL) mixture under blue light irradiation (405 nm) at room temperature. The primary by-products generated from the aerobic degradation process included acetophenone and oxidized PS with a reduced average molecular weight. Notably, different forms of PS waste including cup lids, yogurt containers, loose-fill chips, EPS foam, food boxes, and laboratory weighing boats can be effectively utilized, furnishing the benzoic acid as a pure white crystalline powder in satisfying yields. Moreover, the gram-scale aerobic degradation of PS was further achieved by employing continuous-flow microreactor technology. The desired products were smoothly obtained from the flow degradation of PS by mixing a solution of PS and *p*TsOH·H_2O with oxygen gas at a pressure of 6 bar and a temperature of 70 °C, with 420 nm high power lamp present during the process. Density functional theory (DFT) calculations were conducted using 1,3-diphenylbutane **25** as a model substrate to explore the hydrogen atom transfer between 1,3-diphenylbutane and various reactive oxygen species (ROS), such as singlet oxygen ($^1O_2$), hydroxyl radical ($^{\bullet}OH$), superoxide ion ($O_2^{\bullet-}$), and triplet oxygen ($^3O_2$). Among these, the HAT involving $^1O_2$ occurs through the transition state **TS**, which has the lowest energy barrier ($\Delta G^{\ddagger}$ = 4.8 kcal mol^{-1}). This suggests that $^1O_2$ is the most likely ROS to initiate the degradation of the PS. Consistently, quenching experiments involving $^1O_2$, EPR investigations collectively demonstrate that $^1O_2$ is the reactive oxygen species responsible for the degradation of PS. This process involves the abstraction of a hydrogen atom from a tertiary C–H bond, resulting in hydroperoxidation and subsequent C–C bond cleavage through a radical mechanism. UV-vis absorption experiments indicated that the generation of singlet oxygen in the absence of a photosensitizer is facilitated by a potential polystyrene-acid adduct. The isolated oxidized polystyrene also demonstrated strong absorption at 405 nm, suggesting that the *in situ* formation of oxidized polystyrene enhances its concentration and acts as a photosensitizer. Therefore, the interaction between these components is crucial for the effective generation of reactive oxygen species.

Polystyrene can also undergo aerobic degradation effectively under visible light without the requirement of acid promotion. In 2022, The Das group revealed a photocatalytic method for the selective upcycling of PS waste into benzoic acid, facilitated by NBS/CF_3SO_2Na (Scheme 10).[42] In this process, bromine radicals serve as hydrogen atom transfer (HAT) agents, enhancing the generation of carbon radicals on the polymer backbones in the presence of O_2 atmosphere and under the irradiation of Kessil light (390 nm). With commercial PS (M_w ~ 260 000 g mol^{-1}, M_n ~ 104 000 g mol^{-1}) as the starting material, benzoic acid could be produced with a yield of 73% by employing 15 mol% NBS and 50 mol% CF_3SO_2Na, alongside small amount of benzoyl by-product such as benzoyl bromide, acetophenone and benzaldehyde. The reaction demonstrates high efficiency, as evidenced by the significant reduction in polymer molecular weight from 260 000 g mol^{-1} to 1560 g mol^{-1} within just 2 hours of photoactivation. It is worth noting that the aerobic upcycling of PS is also feasible in the air, albeit with slightly lower efficiency. Thirteen varieties of real-life plastics, both high and low molecular weight, were selectively depolymerized into benzoic acid with yields of up to 68%, regardless of the presence of polymer additives. Notably, the benzoic acid generated from PS degradation can undergo further transformation into benzene, biphenyl, salicylic acid, toluene, and various important bioactive compounds through tandem reactions. This presents a viable alternative to conventional petrochemical feedstocks in the chemical and pharmaceutical sectors. Detailed mechanistic studies elucidated that pentacoordinate sulfide was the actual active species, produced from CF_3SO_2Na in the presence of O_2

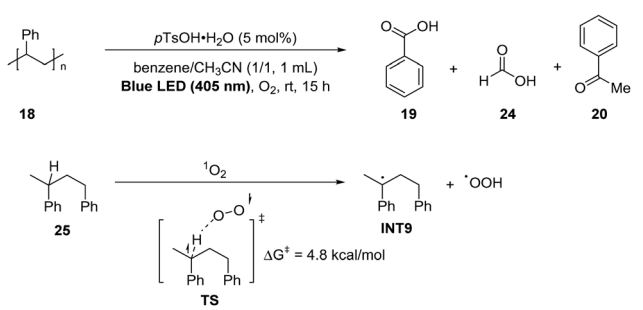

Scheme 9 Acid-catalysed aerobic degradation of polystyrene under visible light.

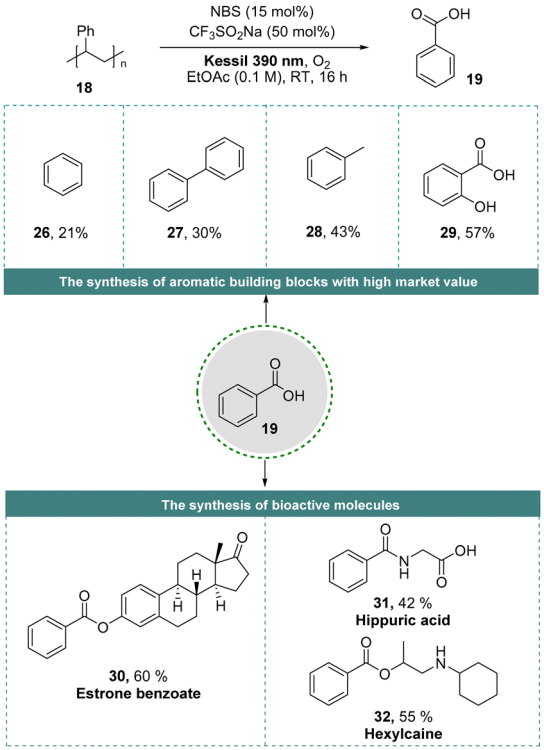

Scheme 10 NBS/CF_3SO_2Na facilitated aerobic degradation of polystyrene under visible light.

and light, which participates in hydrogen atom transfer (HAT) alongside the product of NBS (Scheme 11).

Recently, researchers are increasingly focused on discovering new photocatalysts capable of absorbing visible light to enable photocatalytic oxidative degradation. In 2023, Jiang group disclosed a novel uranyl-photocatalysis enabled

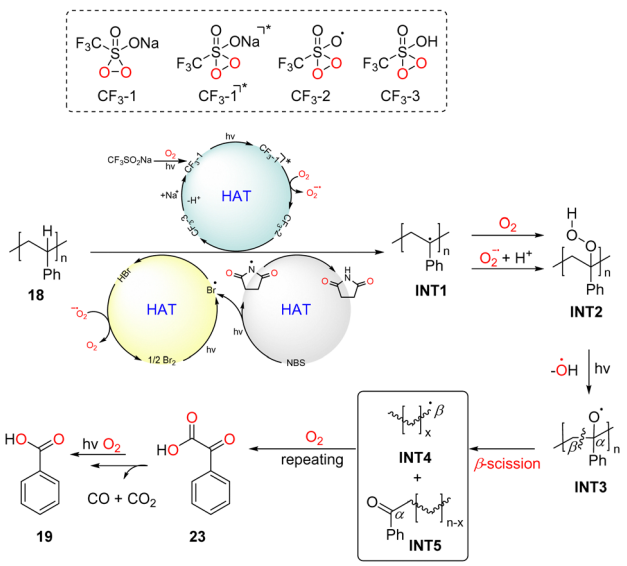

Scheme 11 Possible mechanism for NBS/CF_3SO_2Na facilitated aerobic degradation of polystyrene under visible light.

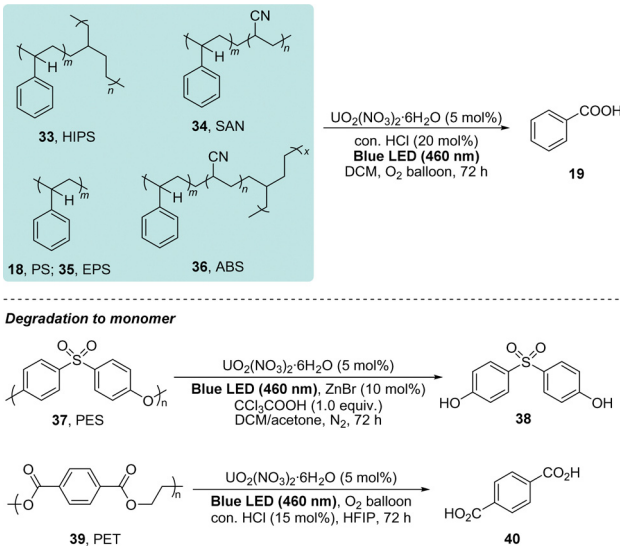

Scheme 12 Degradation of plastic wastes with uranyl-photocatalyst under visible light.

degradation of plastic wastes to commercial chemicals and monomers under visible light (Scheme 12).[43] In this process, irradiating a solution of PS in dichloromethane with blue light (460 nm) in the presence of uranyl nitrate hexahydrate ($UO_2(NO_3)_2·6H_2O$) resulted in the formation of benzoic acid with a yield of 30%, using HCl as an additive. Importantly, five kinds of styrene-based block copolymers, recognized for their strong impact strength and heat stability that contribute to their resistance to degradation, can be effectively depolymerized into benzoic acid with some oligomers. Additionally, these styrene-based block copolymers can be depolymerized into benzoic acid in a mixed waste stream, eliminating the need for sorting plastic waste and enhancing upcycling efficiency. By using different solvents and additives, this approach can also be applied to the degradation of polyethers, polycarbonates, and polyesters. Specifically, polyethersulfone (PES) and polycarbonate (PC) were degraded into the monomers bis(4-hydroxyphenyl)sulfone and bisphenol A, respectively. To showcase the practical application of this method, a continuous flow photoreactor with a 180 mL residue volume was developed for the degradation of kilogram-scale PET bottles. This setup achieved a 54 800-fold increase in efficiency compared to traditional batch operations,[44] yielding terephthalic acid (TPA) in 88% yield within 2 days while using a reduced dosage of catalyst and solvent. Further, the degradation profile was analysed using scanning electron microscopy (SEM) imaging, X-ray diffraction, and gel permeation chromatography (GPC) to trace the degradation process.

For the polystyrene block copolymers and polyesters that yield acidic products, a synergistic mechanism involving single-electron transfer (SET) and hydrogen atom transfer (HAT) processes is proposed (Scheme 13). In this mechanism, the excited state $*UO_2^{2+}$ captures hydrogen radicals from the benzyl site, leading to the formation of carbon radicals. These radicals then undergo peroxidation and bond scission to obtain the

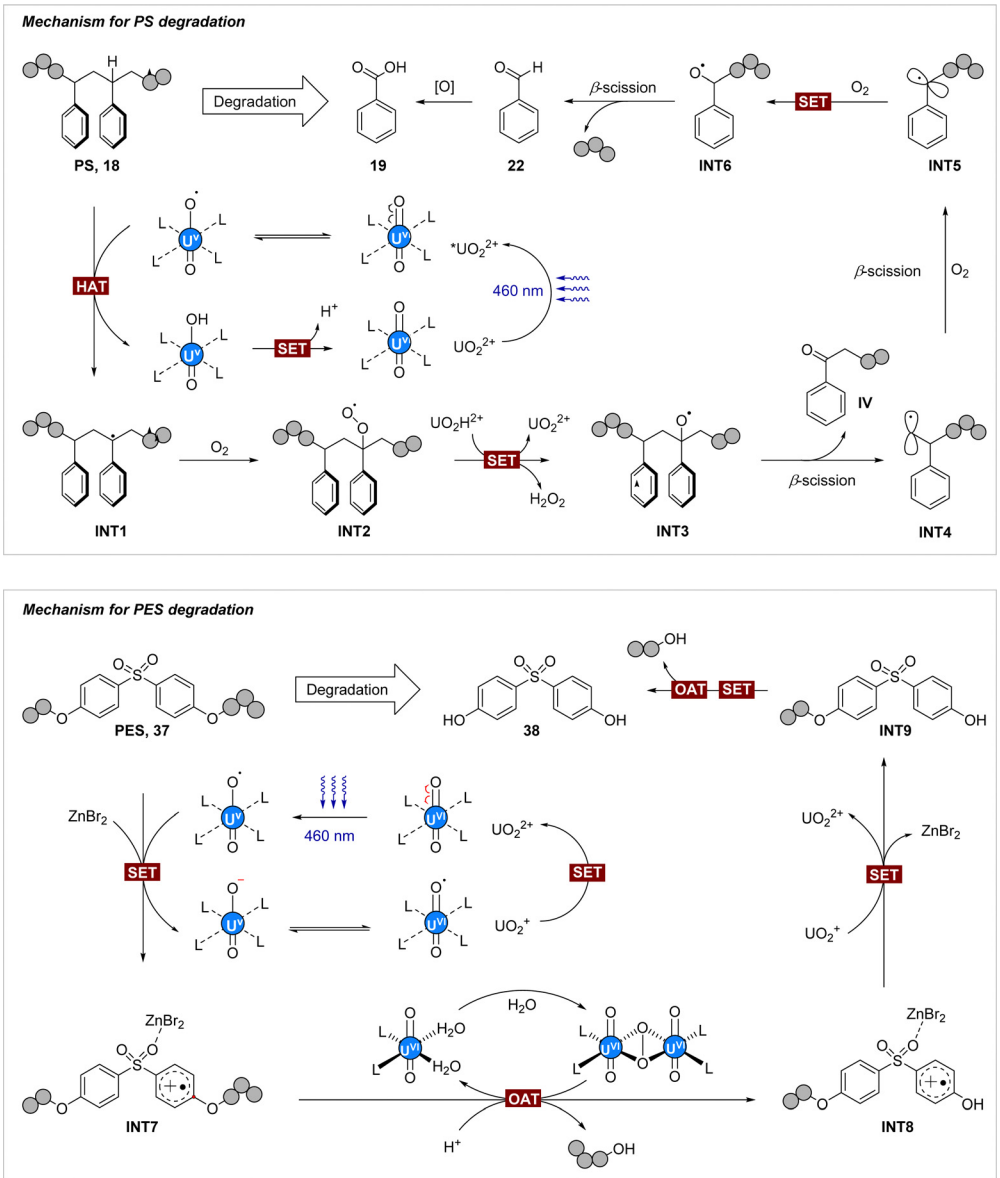

Scheme 13 Possible mechanism for degradation of plastic wastes with uranyl-photocatalyst under visible light.

benzoic acid. In contrast, for polycarbonates and polyethers, a synergistic mechanism involving oxidative addition transfer (OAT) and SET is suggested. Here, the aromatic rings of the polymers are oxidized by the excited state $*UO_2^{2+}$ through the SET process, generating aryl radical cation species. These species then undergo an OAT process followed by a second SET, resulting in the formation of unilateral phenol. Finally, the intermediated will undergo reduplicative OAT and SET sequentially to yield the monomer. Inspired by this work, the Su group recently developed a method for promoting the degradation of PS using blue light or sunlight in conjunction with uranyl photocatalysis.[45] In this approach, ethyl acetate serves as the reaction medium, offering a safer alternative to conventional solvents that are often toxic, volatile, and explosive.

By leveraging the successful cleavage of C–H and C–C bonds achieved through light-driven LMCT involving iron chloride, the next logical step is to extend this knowledge to the oxidative degradation of polymers. In 2021, Zeng and coworkers explored the photoinduced oxidation of alkyl aromatics using $FeCl_3$ as a catalyst and extended this reaction to the degradation of polystyrene.[46] By introducing tetrabutylammonium chloride (TBAC) as additives and 2,2,2-trichloroethanol as HAT catalyst, PS will undergo $FeCl_3$ promoted oxidative degradation under 390 nm light irradiation for 5 days to obtain benzoic acid in 67% yield (Scheme 14(a)). It is important to mention that alkoxy or chlorine radicals can be produced from 2,2,2-trichloroethanol or Cl– *via* photo-induced LMCT. However, the generation of chlorine radicals is favored since the reaction can take place even without alcohol. In 2022, the Stache group reported a similar approach for the degradation of polystyrene.[47] Using a white LED lamp as the light source, they irradiated polystyrene in the presence of $FeCl_3$ in acetone under air for 20 hours.

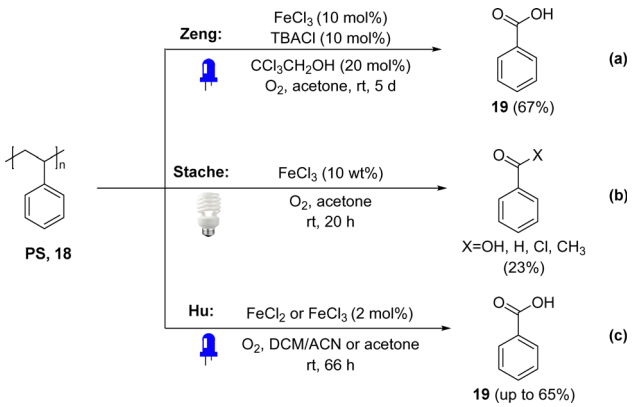

Scheme 14 Photo-induced iron catalysed oxidative degradation of polystyrene.

This process produced polystyrene oligomers (M_n = 0.8 kg mol^{-1}) and small molecules at a yield of 11 mol% (on a per monomer basis), primarily consisting of benzoyl products such as benzoic acid, benzaldehyde, benzoyl chloride, and acetophenone. When the reaction was charged with an oxygen balloon, the formation of benzoyl products can be increased to 23 mol% within 20 h (Scheme 14(b)). Some commercial polystyrene samples were subjected to the standard reaction conditions; however, the degradation resulted in high molecular weights and broad dispersities when measured the Mn and dispersities *via* SEC analysis.[48,49]

The mechanism of these $FeCl_3$-promoted degradations involves the light-induced generation of chlorine radicals, which abstract a hydrogen atom from the polystyrene backbone (Scheme 15). Following the trapping of the polystyrene radical with oxygen, the catalyst is regenerated during the formation of hydroperoxides. This is followed by a reduction process that generates alkoxy radicals **INT4**, leading to irreversible carbon–carbon bond cleavage *via* β-scission and ultimately resulting in the production of benzoic acid.

Hu and co-workers also reported a practical iron catalysed selective degradation of PS under visible light.[50] In this process, two solvent systems (DCM/MeCN, acetone) were employed as ideal media when using $FeCl_2$ as the catalyst under blue LED (Scheme 14(c)). Furthermore, the degradation conditions can be simplified by using sunlight irradiation in the air without the need for a solvent. This photocatalytic protocol is highly efficient for PS particles of varying molecular weights, copolymers of styrene, and commercial plastic waste derived from PS, all of which can be converted into benzoic acid.

Fluorescence quenching experiments with Fe^{III*} suggested that a different mechanism was involved in this process. It was proposed that a carbon radical on the polymer backbone is generated through a single-electron transfer (SET) process with the excited Fe^{III}. The formation of a four-membered ring intermediate,[51] derived from the enol form of the ketone and singlet oxygen, is considered a crucial step in this conversion, which subsequently decomposes to produce benzoic acid as the end product. However, the light-induced ligand-to-metal charge transfer (LMCT) mechanism cannot be ruled out, as TBAC was used as an additive when non-chloride iron salts were employed as the catalyst, and chloride ions are always present in the system.

Recently, the Zeng group reported a Brønsted acid-promoted oxidative degradation of polyethylene terephthalate (PET) into its monomer, ethylene terephthalate, through photoinduced iron catalysis (Scheme 16).[52] Upon irradiation with 390 nm LEDs and in the presence of $FeCl_3$, 50 mol% conc. HCl, and oxygen balloon, PET (25 kDa) can be depolymerized efficiently to give the ethylene terephthalate in up to 97% yield. Remarkably, the catalyst loading can be reduced to just 0.25 mol% while still maintaining high reactivity. Following a simple shredding process, various types of PET waste from daily life can be converted into the monomer *via* the catalytic approach, yielding moderate to high results. Thanks to the presence of weaker C–H bonds located next to the oxygen atoms within the polymer chains, it is possible to selectively depolymerize PET from mixed plastics. Preliminary control experiments and UV-vis studies suggested that HCl engaged in the formation of reactive species $[Fe(III)Cl_4]^-$ in the presence of $FeCl_3$ to facilitate the light induced LMCT (Scheme 17). The resulting chlorine radicals will capture a hydrogen atom from the site adjacent to

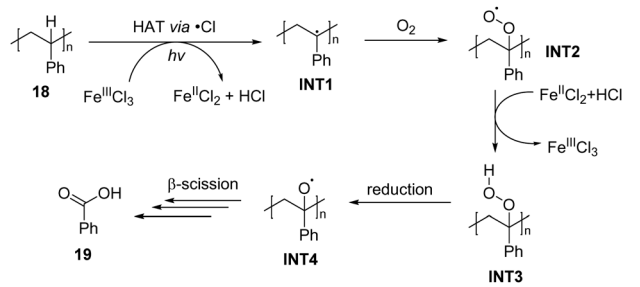

Scheme 15 Possible mechanism of $FeCl_3$-promoted degradations under visible light.

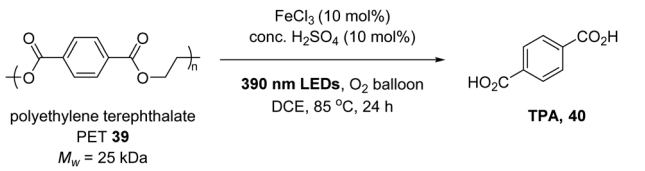

Scheme 16 Photo-induced iron catalyzed oxidative degradation of polyethylene terephthalate.

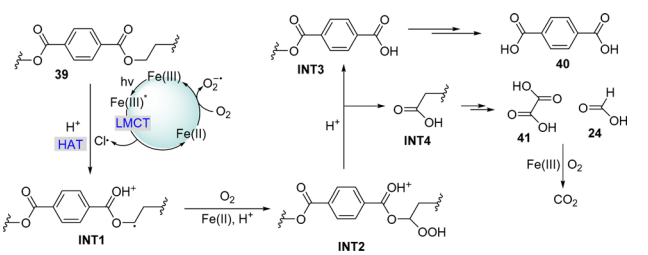

Scheme 17 Possible mechanism for photo-induced iron catalysed oxidative degradation of PET.

the oxygen atoms, generating carbon radical **INT1** on the backbone that participates in the subsequent oxidative degradation. The ethylene glycol moiety of PET underwent extensive oxidation, leading to the formation of oxalic acid or formic acid, which ultimately decomposes into carbon dioxide (CO_2).

In a similar approach to facilitating polystyrene degradation by generating chlorine radicals that extract hydrogen atoms through photocatalysis, the Lim group created a fluorinated acridinium photocatalyst. This work involved a combination of experimental and computational methods for screening catalysts aimed at the aerobic degradation of PS. The reaction reactivity can be preserved at low catalyst loadings of less than 5 mol%. Moreover, real-life PS waste that contain dyes and additives are suitable for this degradation process.[53]

The aforementioned initiatives have primarily focused on polystyrene due to the relative ease of activating its C–H bonds. In contrast, the effective and widespread photocatalytic upcycling of polyethylene (PE), polyvinyl chloride (PVC), polypropylene (PP), and other conventional plastics has not yet been resolved, largely because of their significantly higher bond dissociation energies (BDEs). To tackle this issue, the Soo group has developed a degradation approach utilizing commercially available homogeneous vanadium photocatalysts (Scheme 18).[54] Irradiating polystyrene (M_w 35 000) with 2 mol% $V(O)(acac)_2$ in DCM for 5 days under an O_2 atmosphere resulted in the highest yields of formic acid (43.6%), benzoic acid (38.4%), and acetophenone (6.4%). The CHN elemental analyses of the oligomeric residue, combined with HSQC NMR data and FTIR spectroscopy, demonstrated a considerable reduction in the majority of the aliphatic C–H bonds present in the original polystyrene. Noteworthily, three practical methods to preprocess the poorly soluble plastics were provided in detail. Under the established conditions, a wide range of common conventional plastics, including HDPE, LDPE, PVC, PP, PS, (polyvinyl acetate) PVAc, and (ethylene-vinyl acetate copolymer) EVA, proved to be potent substrates, yielding modest to good amounts of carboxylic acid products. Moreover, plastic wastes from post-consumer multilayered packaging, styrofoam, and PP food containers are also suitable for depolymerization. A continuous segmented flow photoreactor, featuring a horizontal spiral of quartz coils, was assembled for the degradation of polymers on a gram scale, allowing for higher concentrations of plastic degradation within

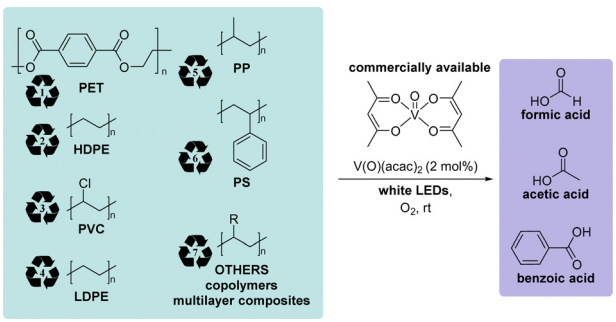

Scheme 18 Photo-induced oxidative degradation of polymers with vanadium photocatalysts.

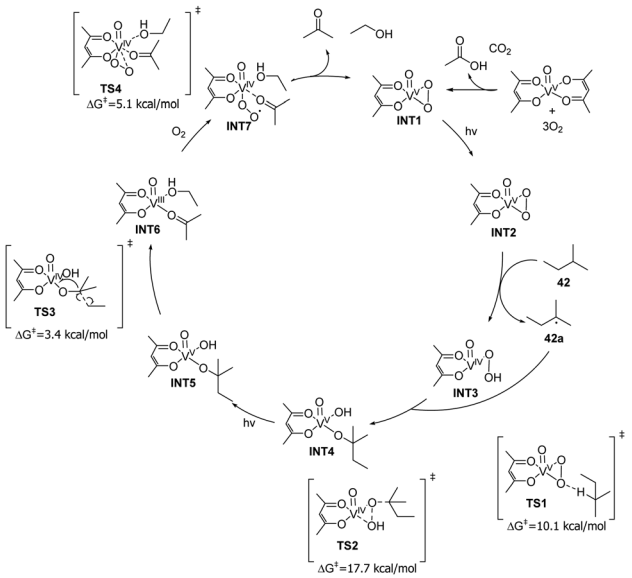

Scheme 19 Proposed mechanism for photo-induced oxidative degradation of polymers with vanadium photocatalysts.

a comparable duration. The presence of both V(v) and V(iv) during the photocatalytic conversion was confirmed through UV-Vis spectroscopy, electron paramagnetic resonance (EPR) spectroscopy, and X-ray photoelectron spectroscopy (XPS).

Furthermore, kinetic studies of the photocatalytic oxidation reaction were performed using *sec*-butylbenzene as a representative substrate. The results showed that the conversion of *sec*-butylbenzene displayed first-order relationships with the concentrations of the substrate, the catalyst, the partial pressure of O_2, and the light flux. The first-order dependence on O_2 concentration indicates that increasing O_2 levels enhances the yields of carboxylate products. DFT calculations were performed using isopentane as a model for polypropylene. The formation of intermediate **INT1** occurs through the oxidation of $V(O)(acac)_2$ by O_2, which is initiated by photoexcitation *via* LMCT (Scheme 19). Subsequently, **INT2** participates in the C–H oxidation of isopentane through transition state TS1, characterized by a low activation barrier of just 10.1 kcal mol^{-1}. The alkyl radical produced from this step can then react with the V^{IV} intermediate **INT3**, overcoming a barrier of 17.7 kcal mol^{-1} and leading to the formation of INT4. Additionally, the photoexcitation of INT4 *via* LMCT facilitates the desired C–C cleavage with a minimal barrier of only 3.4 kcal mol^{-1}, resulting in the production of INT6. Finally, oxidation of INT6 with O_2, along with the dissociation of carbonyl and alcohol products, regenerate **INT1** with a very low barrier of just 5.1 kcal mol^{-1}.

Conclusions

This review mainly summarize the recent advances in chemical upcycling of polymers under visible light irradiation *via* C–H bond activation. Based on different reaction types, this review is mainly divided into two sections: photochemical C–H functionalization of polymers and photochemical oxidative polymer

degradation. In each section, the reaction mechanisms, compatibility as well as practical application have been emphatically discussed. In contrast to the conventional thermocatalytic approach for polymer upcycling, photocatalytic approach is considered as a more environmentally friendly and cost-effective alternative. These methods operate under mild conditions and exhibit good reactivity, enabling the selective conversion of plastic waste into value-added molecules or high-performance materials.

Despite these significant advances, challenges remain in this field. In photochemical oxidative degradation, polystyrene has primarily been upcycled to produce value-added organic molecules such as benzoic acid. In contrast, widely used plastics with higher BDEs, such as polypropylene and polyethylene, currently lack sufficient methods for achieving efficient and selective degradation, not to mention the degradation of copolymers. Addressing this challenge requires future research to explore new catalysts and reaction conditions that can enhance the degradation efficiency of these more resilient polymers. Besides, numerous current strategies rely on hazardous solvents like benzene and chloroform, as well as corrosive catalysts such as sulfuric acid. This situation highlights the urgent necessity to create safer and more sustainable alternatives. In the photochemical modification of polymers, the exploration of new methods for C–H functionalization is essential for future development. Meanwhile, there is a strong demand for the development of more efficient and cost-effective photocatalysts to facilitate chemical upcycling with enhanced selectivity. Additionally, photo-induced synergistic catalysis may provide new opportunities to expand the range of upcycling methods.

While photochemical upcycling technologies show promising results in small-scale laboratory tests, several challenges arise when applying them at an industrial scale, including reactor design, catalyst stability, and optimization of reaction conditions. For instance, the choice of light source, control of reaction temperature, and pressure require meticulous adjustments to suit large-scale production needs. In industrial applications, the continuity and stability of the reaction process are critical. Factors such as catalyst lifecycle management, the purity of reactants, and control of reaction time all need careful consideration. Additionally, the investment and maintenance costs of industrial equipment must be factored in to ensure the economic viability of the technology. Innovations in the laboratory often struggle to be directly translated into commercial applications. To address this, interdisciplinary collaboration mechanisms involving chemical engineering, materials science, and industrial design are needed to facilitate the development and optimization of technologies. Technologies that succeed in the laboratory need to undergo multiple rounds of prototype development and testing to ensure their effectiveness and reliability in actual production.

Photochemical upcycling of polymers not only provide effective solutions to reduce plastic pollution but also offer potential pathways to achieve circular economy goals. We hope this highlight will inspire chemists to pursue further advancements, develop innovative methods for polymer upcycling, and achieve large-scale applications to address plastic pollution.

Data availability

No primary research results, software or code have been included and no new data were generated or analysed as part of this review.

Conflicts of interest

There are no conflicts to declare.

Acknowledgements

The authors thank the Natural Science Foundation of China (no. 22271314, 22401295), the fundamental research funds for the central universities of South-Central MinZu University (CZH23004, CZH24004) for financial support, the fundamental research funds for Academic Innovation Teams of South-Central Minzu University (grant number: XTZ24015).

Notes and references

1 N. P. Ivleva, *Chem. Rev.*, 2021, **121**, 11886–11936.
2 (*a*) J. H. Li, *Sci. Technol. Rev.*, 2024, **42**, 1–2; (*b*) A. Kulkarni, G. Quintens and L. M. Pitet, *Macromolecules*, 2023, **56**, 1747–1758.
3 J. R. Jambeck, R. Geyer, C. Wilcox, T. R. Siegler, M. Perryman, A. Andrady, R. Narayan and K. L. Law, *Science*, 2015, **347**, 768–771.
4 United Nations Environment Programme, *From Pollution to Solution: A global assessment of marine litter and plastic pollution*, ed. J. Smith, Nairobi, 2021.
5 (*a*) S. Al-Salem, P. Lettieri and J. Baeyens, *Waste Manage.*, 2009, **29**, 2625–2643; (*b*) J. Lange, S. R. A. Kersten, S. De Meester, M. C. P. van Eijk and K. Ragaert, *ChemSusChem*, 2024, **17**, e202301320; (*c*) B. Zhao, Z. Hu, Y. Sun, R. Hajiayi, T. Wang and N. Jiao, *J. Am. Chem. Soc.*, 2024, **146**, 28605–28611; (*d*) B. Zhao, H. Tan, J. Yang, X. Zhang, Z. Yu, H. Sun, J. Wei, X. Zhao, Y. Zhang, L. Chen, D. Yang, J. Deng, Y. Fu, Z. Huang and N. Jiao, *Innovation*, 2024, **5**, 100586.
6 Z. O. G. Schyns and M. P. Shaver, *Macromol. Rapid Commun.*, 2020, **42**, 2000415.
7 D. V. A. Ceretti, M. Edeleva, L. Cardon and D. R. D'hooge, *Molecules*, 2023, **28**, 2344.
8 L. D. Ellis, N. A. Rorrer, K. P. Sullivan, M. Otto, J. E. McGeehan, Y. Román-Leshkov, N. Wierckx and G. T. Beckham, *Nat. Catal.*, 2021, **4**, 539–556.
9 L. Zhang, Z. Bao, S. Xia, Q. Lu and K. B. Walters, *Catalysts*, 2018, **8**, 659.
10 N. De Alwis Watuthanthrige, R. Whitfield, S. Harrisson, N. P. Truong and A. Anastasaki, *ACS Macro Lett.*, 2024, **13**, 806–811.
11 K. Thielemans, Y. De Bondt, S. Van den Bosch, A. Bautil, C. Roye, A. Deneyer, C. M. Courtin and B. F. Sels, *Carbohydr. Polym.*, 2022, **294**, 119764.
12 J. Aguado, D. P. Serrano and J. M. Escola, *Ind. Eng. Chem. Res.*, 2008, **47**, 7982–7992.
13 F. Eisenreich, *Angew. Chem., Int. Ed.*, 2023, **62**, e202301303.
14 (*a*) M. Zhang, R. H. Colby, S. T. Milner, T. C. M. Chung, T. Huang and W. deGroot, *Macromolecules*, 2013, **46**, 4313–4323; (*b*) P. Tiwary and C. Guria, *J. Polym. Environ.*, 2010, **18**, 298–307.
15 (*a*) S. Chu, B. Zhang, X. Zhao, H. S. Soo, F. Wang, R. Xiao and H. Zhang, *Adv. Energy Mater.*, 2022, **12**, 2200435; (*b*) C. Zhang, Q. Kang, M. Chu, L. He and J. Chen, *Trends Chem.*, 2022, **4**, 822–834; (*c*) M. R. Karimi Estahbanati, X. Y. Kong, A. Eslami and H. S. Soo, *ChemSusChem*, 2021, **14**, 4152–4166; (*d*) K. Parkatzidis, H. S. Wang and A. Anastasaki, *Angew. Chem., Int. Ed.*, 2024, **63**, e202402436; (*e*) P. Z. Wang, W. J. Xiao and J. R. Chen, *Nat. Rev. Chem.*, 2022, **7**, 35–50; (*f*) X. Y. Yu, J. R. Chen and W. J. Xiao, *Chem. Rev.*, 2020, **121**, 506–561.
16 C. K. Prier, D. A. Rankic and D. W. C. MacMillan, *Chem. Rev.*, 2013, **113**, 5322–5363.

17 (*a*) S. Oh and E. E. Stache, *Chem. Soc. Rev.*, 2024, **53**, 7309–7327; (*b*) Q. Y. Lee and H. Li, *Micromachines*, 2021, **12**, 907.
18 (*a*) L. Capaldo, D. Ravelli and M. Fagnoni, *Chem. Rev.*, 2021, **122**, 1875–1924; (*b*) L. Capaldo, L. L. Quadri and D. Ravelli, *Green Chem.*, 2020, **22**, 3376–3396.
19 B. Obermeier, F. Wurm, C. Mangold and H. Frey, *Angew. Chem., Int. Ed.*, 2011, **50**, 7988–7997.
20 (*a*) A. S. Belousov and I. Shafiq, *J. Environ. Chem. Eng.*, 2023, **11**, 110970; (*b*) Y. Xu, Y. Lin, S. L. Homölle, J. C. A. Oliveira and L. Ackermann, *J. Am. Chem. Soc.*, 2024, **146**, 24105–24113; (*c*) J. Zhang and M. Rueping, *Nat. Catal.*, 2024, **7**, 963–976.
21 (*a*) Z. Ouyang, Y. Yang, C. Zhang, S. Zhu, L. Qin, W. Wang, D. He, Y. Zhou, H. Luo and F. Qin, *J. Mater. Chem. A*, 2021, **9**, 13402–13441; (*b*) W. Li, W. Zhao, H. Zhu, Z. J. Li and W. Wang, *J. Mater. Chem. A*, 2023, **11**, 2503–2527; (*c*) J. Sun, J. Dong, L. Gao, Y. Q. Zhao, H. Moon and S. L. Scott, *Chem. Rev.*, 2024, **124**, 9457–9579.
22 J. B. Williamson, S. E. Lewis, R. R. Johnson, I. M. Manning and F. A. Leibfarth, *Angew. Chem., Int. Ed.*, 2019, **58**, 8654–8668.
23 O. G. Mountanea, E. Skolia and C. G. Kokotos, *Green Chem.*, 2024, **26**, 8528–8549.
24 (*a*) S. Chu, B. Zhang, X. Zhao, H. S. Soo, F. Wang, R. Xiao and H. Zhang, *Adv. Energy Mater.*, 2022, **12**, 2200435; (*b*) X. Tang, X. Han, N. H. M. Sulaiman, L. He and X. Zhou, *Ind. Eng. Chem. Res.*, 2023, **62**, 9032–9045.
25 J. B. Williamson, W. L. Czaplyski, E. J. Alexanian and F. A. Leibfarth, *Angew. Chem., Int. Ed.*, 2018, **57**, 6261–6265.
26 P. Gloor, Y. Tang, A. Kostanska and A. Hamielec, *Polymer*, 1994, **35**, 1012–1030.
27 (*a*) W. Zhou, X. Wu, M. Miao, Z. Wang, L. Chen, S. Shan, G. Cao and D. Yu, *Chem. – Eur. J.*, 2020, **26**, 15052–15064; (*b*) Q. Dou, T. Wang, L. Fang, H. Zhai and B. Cheng, *Chin. J. Org. Chem.*, 2023, **43**, 1386; (*c*) F. Juliá, *ChemCatChem*, 2022, **14**, e202200916; (*d*) G. D. Xia, R. Li, L. Zhang, Y. Wei and X. Q. Hu, *Org. Lett.*, 2024, **26**, 3703–3708; (*e*) L. J. Li, Y. Wei, Y. L. Zhao, Y. Gao and X. Q. Hu, *Org. Lett.*, 2024, **26**, 1110–1115; (*f*) G. D. Xia, Z. K. Liu, Y. L. Zhao, F. C. Jia and X. Q. Hu, *Org. Lett.*, 2023, **25**, 5279–5284.
28 T. Xue, Z. Zhang and R. Zeng, *Org. Lett.*, 2022, **24**, 977–982.
29 (*a*) J. L. Tu, A. M. Hu, L. Guo and W. Xia, *J. Am. Chem. Soc.*, 2023, **145**, 7600–7611; (*b*) Y. Jin, L. Wang, Q. Zhang, Y. Zhang, Q. Liao and C. Duan, *Green Chem.*, 2021, **23**, 9406–9411; (*c*) G. D. Xia, R. Li, L. Zhang, Y. Wei and X. Q. Hu, *Org. Lett.*, 2024, **26**, 3703–3708.
30 Z. Zhang, X. Li, D. Zhou, S. Ding, M. Wang and R. Zeng, *J. Am. Chem. Soc.*, 2023, **145**, 7612–7620.
31 Z. Zhang, Y. Zhang and R. Zeng, *Chem. Sci.*, 2023, **14**, 9374–9379.
32 I. D. Jurberg and H. M. L. Davies, *Chem. Sci.*, 2018, **9**, 5112–5118.
33 H. M. L. Davies and J. R. Manning, *Nature*, 2008, **451**, 417–424.
34 S. Yi, S. Yang, Z. Xie, J. Yun and X. Pan, *ACS Macro Lett.*, 2024, **13**, 711–718.
35 J. W. Beatty, J. J. Douglas, K. P. Cole and C. R. J. Stephenson, *Nat. Commun.*, 2015, **6**, 7919.
36 S. E. Lewis, B. E. Wilhelmy and F. A. Leibfarth, *Chem. Sci.*, 2019, **10**, 6270–6277.
37 S. E. Lewis, B. E. Wilhelmy and F. A. Leibfarth, *Polym. Chem.*, 2020, **11**, 4914–4919.
38 (*a*) A. Andrady, P. Barnes, J. Bornman, T. Gouin, S. Madronich, C. White, R. Zepp and M. Jansen, *Sci. Total Environ.*, 2022, **851**, 158022; (*b*) O. Chiantore, L. Trossarelli and M. Lazzari, *Polymer*, 2000, **41**, 1657–1668.
39 T. Li, A. Vijeta, C. Casadevall, A. S. Gentleman, T. Euser and E. Reisner, *ACS Catal.*, 2022, **12**, 8155–8163.
40 N. F. Nikitas, E. Skolia, P. L. Gkizis, I. Triandafillidi and C. G. Kokotos, *Green Chem.*, 2023, **25**, 4750–4759.
41 Z. Huang, M. Shanmugam, Z. Liu, A. Brookfield, E. L. Bennett, R. Guan, D. E. Vega Herrera, J. A. Lopez-Sanchez, A. G. Slater, E. J. L. McInnes, X. Qi and J. Xiao, *J. Am. Chem. Soc.*, 2022, **144**, 6532–6542.
42 Y. Qin, T. Zhang, H. V. Ching, G. S. Raman and S. Das, *Chem*, 2022, **8**, 2472–2484.
43 J. Meng, Y. Zhou, D. Li and X. Jiang, *Sci. Bull.*, 2023, **68**, 1522–1530.
44 D. Cambié, C. Bottecchia, N. J. W. Straathof, V. Hessel and T. Noël, *Chem. Rev.*, 2016, **116**, 10276–10341.
45 S. B. Tang, Y. X. Jiang, K. Li, Z. X. Wang and J. Su, *Ind. Eng. Chem. Res.*, 2024, **63**, 4817–4824.
46 G. Zhang, Z. Zhang and R. Zeng, *Chin. J. Chem.*, 2021, **39**, 3225–3230.
47 S. Oh and E. E. Stache, *J. Am. Chem. Soc.*, 2022, **144**, 5745–5749.
48 S. Oh and E. E. Stache, *ACS Catal.*, 2023, **13**, 10968–10975.
49 D. L. Langer, S. Oh and E. E. Stache, *Chem. Sci.*, 2024, **15**, 1840–1845.
50 M. Wang, J. Wen, Y. Huang and P. Hu, *ChemSusChem*, 2021, **14**, 5049–5056.
51 (*a*) S. K. Silverman and C. S. Foote, *J. Am. Chem. Soc.*, 1991, **113**, 7672–7675; (*b*) A. P. Schaap, K. A. Zaklika, B. Kaskar and L. W. M. Fung, *J. Am. Chem. Soc.*, 1980, **102**, 389–391.
52 S. Wang, L. Wang, T. Xue, G. Zhang, C. Ke and R. Zeng, *Chin. J. Chem.*, 2024, **42**, 2431–2437.
53 A. Ong, Z. C. Wong, K. L. O. Chin, W. W. Loh, M. H. Chua, S. J. Ang and J. Y. C. Lim, *Chem. Sci.*, 2024, **15**, 1061–1067.
54 C. Li, X. Y. Kong, M. Lyu, X. T. Tay, M. Đokić, K. F. Chin, C. T. Yang, E. K. X. Lee, J. Zhang, C. Y. Tham, W. X. Chan, W. J. Lee, T. T. Lim, A. Goto, M. B. Sullivan and H. S. Soo, *Chem*, 2023, **9**, 2683–2700.

